Talanta 253 (2023) 124019

Contents lists available at ScienceDirect

Talanta

journal homepage: www.elsevier.com/locate/talanta

A bespoke reagent-free amperometric bromide sensor for seawater

Yuqi Chen, Richard G. Compton *

Department of Chemistry, Physical and Theoretical Chemistry Laboratory, Oxford University, South Parks Road, Oxford, OX1 3QZ, UK

ARTICLE INFO

Keywords:
Bromide quantification
Amperometry
Platinum electrode
Standard additions
Electrochemical analysis
Seawater

ABSTRACT

Measurement of the exact concentration of bromide in seawater, usually present at the ca milli-Molar level, is significant for evaluating geological, biological and environmental conditions. Although silver electrodes are commonly used for amperometric halide measurements, providing selectivity for the ions with similar concentrations, the bromide signal obtained in seawater is masked by that of chloride at hundred millimolar levels. Thus, an alternative bespoke reagent-free electrochemical bromide sensor for seawater was developed with the benefits of low cost, simplicity and rapidity. This is based on the voltammetric oxidation of bromide at Pt macroelectrode, which results in a well-defined signal that is separated from the chloride oxidation peak in seawater. The sensitive quantification was performed by square wave voltammetry combined with the standard addition method, which was evidenced to be valid in both artificial seawater and authentic natural seawater. The measured bromide concentrations of three real samples show good agreement with the results obtained by ion chromatography.

1. Introduction

71% of the earth's surface is covered by the ocean, while 96.5% of the known water on the earth consists of seawater [1]. Human activities are changing the ocean through eutrophication, pollution, warming, acidification, deoxygenation, and nutrient flux reduction amongst other concerns [2,3]. For example, the decrease in the pH of seawater from 8.2 to 8.1 is thought to have resulted from the Industrial Revolution, and arises from the increased formation of carbonic acid due to more carbon dioxide emissions (Eqn (1)) [4].

$$CO_2 + H_2O \rightarrow H_2CO_3 \quad (1)$$

Conversely, the physical and chemical parameters of seawater can be used to track its condition and monitor anthropogenically induced alterations, which is essential to assist regulating societal and industrial development. Usually, seawater contains only a trace of bromide being present at ca milli-Molar concentrations, but information about exact levels is important for evaluating geological, biological and environmental conditions. For example, the levels of bromide ions in the surface and ground waters near the sea are greatly changed by and indicative of seawater intrusion [5]. Further, bromide can be converted to the reactive gas species, bromine (Br_2) and to hypobromous acid (HOBr), leading to surface ozone depletion via the chemistry summarised in Fig. 1 [6]. Note that the sequence of reactions $Br + O_3 \rightarrow BrO + O_2$ followed by $BrO + BrO \rightarrow 2Br + O_2$ indicates a catalytic loss mechanism for ozone [6]. Importantly, bromide is naturally present in fossil fuels, notably coal, so environmental trends due to fossil fuel activities are reflected in concentration changes of bromide in surface seawater [7]. Furthermore, as a result of industrial wastewater discharge, bromide can combine with organic pollutants forming toxic compounds including bromoacetonitriles, bromoacetamides and bromonitromethanes [7–9]. Finally, we note that a high concentration of bromide itself can be toxic to humans. All these factors emphasise the importance of bromide detection in seawater [10,11]

Table 1 shows the essential composition of seawater [12], and that chloride is the most dominant anion. In contrast, bromide has a typical concentration of just 0.86 mM, which is much lower than that of chloride. Although the local concentrations of chloride and bromide depend on location and season [13,14], the ratio between them in normal seawater mostly stays relatively constant (being around 300:1 w/w) [15,16] and indeed the chloride ion concentration is sometimes used to give approximate estimates of bromide levels, although this risks errors where usual levels of bromide exist. Thus, to successfully measure the concentration of bromide, the potential interference by Cl^- present at hundred millimolar levels must be considered.

Current bromide detection and quantification techniques include kinetic-spectrophotometric [5,17–23], chromatography [24,25], capillary electrophoresis [26–30] and electrochemistry [31–34]. Several

* Corresponding author.
E-mail addresses: yuqi.chen@sjc.ox.ac.uk (Y. Chen), richard.compton@chem.ox.ac.uk (R.G. Compton).

https://doi.org/10.1016/j.talanta.2022.124019
Received 22 August 2022; Received in revised form 4 October 2022; Accepted 12 October 2022
Available online 19 October 2022

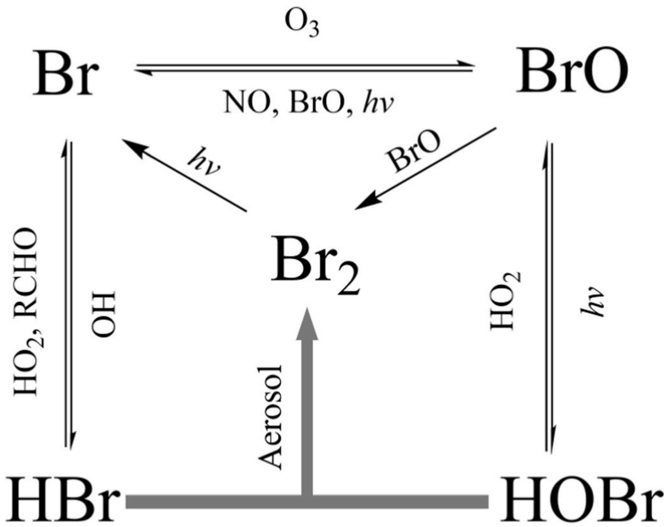

Fig. 1. Schematic reaction diagram of bromide. Thin lines indicate gas-phase reactions. The thick lines show an aerosol reaction [6].

Table 1
Concentrations of major ions in surface seawater [12].

Ion	Molar Concentration/mM
Na^{+}	4.81×10^{2}
Mg^{2+}	5.41×10^{1}
Ca^{2+}	1.05×10^{1}
K^{+}	1.05×10^{1}
Sr^{2+}	9.20×10^{-2}
Cl^{-}	5.59×10^{2}
SO_4^{2-}	2.89×10^{1}
HCO_3^{-}	1.89
CO_3^{2-}	1.89×10^{-1}
Br^{-}	8.63×10^{-1}
$B(OH)_4^{-}$	8.39×10^{-2}
$B(OH)_3$	3.42×10^{-1}
F^{-}	7.00×10^{-2}

studies on bromide detection using the kinetic-spectrophotometric method have been reported [5,17–23]. In this approach a strong oxidising agent such as chloramine T (CT) is commonly used for the formation of OBr^{-} from bromide, followed by a reaction with an indicator resulting in a colour change, e.g. from converting phenol red to bromophenol blue [17]. However, the presence of other ions that can react with the oxidising agent is always a concern. For example, apart from hydroxylamine (NH_2OH) that can be found in the ground, surface waters, and coastal water albeit with lower concentrations [17,35,36], other halide ions, especially chloride in seawater, present significant interferences [5,21]. Meanwhile, the sensitivity of some methods is temperature dependent [22,23] or the dilution of samples is required [5].

In addition to kinetic-spectrophotometric method, chromatography [24,25] combined with a suitable detector is one of the 'gold standards' for sample quantification. For example, ion chromatography is specifically recommended by CEN and ISO [37] for the analysis of drinking water. However, the method requires expensive instruments and time-consuming procedures, including repeated calibration and dilution of the analyte [38]. Capillary electrophoresis is often applied for bromide detection in medicine [26,27] and analysis of human serum [28] has been reported, while the application in seawater has been studied by Fukushi et al. [29] and Kocatürk et al. [30]. Even though CE is a good alternative to IC due to shorter sample preparation and analysis time, smaller reagent consumption and cheaper fused silica capillaries used instead of chromatographic columns [30], electrochemistry may nevertheless prove a better option, offering benefits of low cost, simplicity and rapidity with comparable selectivity.

Potentiometry is widely applied as an electrochemical technique for bromide detection. In particular, the use of a bromide ion-selective electrode (Br-ISE) has been reported in several studies [31–34]. However, if the electrode is developed from scratch, the fabrication procedure is often complex and a preconditioning step may also be required. Zahran et al. reported PVC-membrane cocktails consisting of different compositions requiring optimisation [32], while the whole process was found to be time-consuming, subject to inconsistent manual fabrication methods, difficult for manufacture in small sizes as well as the electrodes having short lifetimes [39]. For example, a Br-ISE based on a silver bromide membrane needs to be preconditioned by 48 h of soaking in 0.01 M KBr solutions [40]. Moreover, though these bespoke electrodes reported by Zahran et al. and Rechnitz et al. are nominally bromide selective, the selectivity coefficient towards Cl^{-} is about 10^{-2} [32,40], which is not sufficient for seawater with the presence of chloride in hundreds of millimolar in comparison with the sub millimolar levels of bromide. Whilst there are many commercially available potentiometric sensors [41–43], they are subject to interference from other ions, notably and for example Cl^{-}, I^{-}, S^{2-}, CN^{-} and strong reducing agents. For example, the description of ECD S80 Bromide Sensors [43] emphasises that Cl^{-}, I^{-} and S^{2-} will form insoluble precipitates on the electrode surface diminishing the response. Commercial ISEs are also costly. More generally, the logarithmic relation between potential and bromide activity results in a change of signal of a mere ca 60 mV per decade of concentration at 298 K, which makes it challenging to deliver a precise and sensitive detection by potentiometry. Meanwhile, there is no guarantee of the quantification accuracy, especially in complex matrixes with the risk of interference or malfunction/fouling of electrodes. However, an amperometric measurement via voltammetry provides a possible alternative robust and inexpensive, reagent-free method for bromide detection. To be more specific, silver-based electrodes are commonly used for bromide, or general halide measurements [44–46], based on the chemistry shown in equation (2):

$$AgX(s) + e^{-} \rightleftharpoons Ag + X^{-} \tag{2}$$

where $X = Cl^{-}$, Br^{-} and I^{-}. Several literature reports [47,48] have stated that Cl^{-}, Br^{-} and I^{-} with similar concentrations can be selectively detected by using silver electrodes, as the deposition peaks of each silver halide occur at different formal potentials (Eqns (3)–(5)) [49]:

$$AgCl + e^{-} \rightleftharpoons Ag + Cl^{-}; E_{Ag/AgCl} = 0.2223 \text{ V } vs. \text{ SCE} \tag{3}$$

$$AgBr + e^{-} \rightleftharpoons Ag + Br^{-}; E_{Ag/AgBr} = 0.0711 \text{ V } vs. \text{ SHE} \tag{4}$$

$$AgI + e^{-} \rightleftharpoons Ag + I^{-}; E_{Ag/AgI} = -0.1522 \text{ V } vs. \text{ SHE} \tag{5}$$

However, in real samples, most importantly seawater with chloride concentration significantly higher than bromide, the bromide signal is masked by the much larger chloride signal as reported below. In order to replace the use of silver electrodes in the context of seawater, we explore other electrode materials notably a platinum electrode that can selectively quantify the bromide concentration despite the high concentration of chloride in seawater.

2. Experimental Section

2.1. Chemicals and reagents

Solutions were prepared using deionised water with a resistivity of 18.2 MΩ cm at 298 K (Millipore, Millipak Express 20, Watford, U.K.). All chemicals were of analytical grade and were used as received without any further purification. Following a literature recipe [50], artificial seawater (ASW) was prepared with the composition of which is presented in Table 2. Sodium chloride (NaCl, 99.5%), potassium chloride (KCl, 99.5%), magnesium chloride dihydrate ($MgCl_2 . 6H_2O$, 99.0%),

Table 2
Chemical composition of synthetic seawater [50].

Composition	Molar Concentration (mol dm^{-3})
NaCl	4.20×10^{-1}
KCl	9.39×10^{-2}
$MgCl_2 . 6H_2O$	5.46×10^{-2}
$CaCl_2 . 2H_2O$	1.05×10^{-2}
$SrCl_2 . 6H_2O$	6.38×10^{-5}
Na_2SO_4	2.88×10^{-2}
$NaHCO_3$	2.38×10^{-3}
KBr	8.40×10^{-4}
NaF	7.15×10^{-5}
H_3BO_3	4.85×10^{-5}

calcium chloride dihydrate ($CaCl_2 . 2H_2O$, 99.0%), strontium chloride hexahydrate ($SrCl_2 . 6H_2O$, 99.0%), sodium sulfate (Na_2SO_4, 99.0%), potassium bromide (KBr, 99.0%), sodium fluoride (NaF, 99.0%) and boric acid (H_3BO_3, 99.5%) were purchased from Sigma-Aldrich, UK, while sodium bicarbonate ($NaHCO_3$, 99.7%) was purchased from Acros Organics, UK. Potassium nitrate (KNO_3, ≥99%) served as a supporting electrolyte was purchased from Sigma-Aldrich, UK.

2.2. Electrochemical apparatus and methods

Electrochemical measurements were performed using a μAutolab II potentiostat (Metrohm-Autolab BV, Utrecht, Netherlands). A standard three-electrode set-up was used in a Faraday cage, being thermostated at a constant value of 25.0 ± 0.2 °C. A graphite rod always served as the counter electrode in all experiments. Either a mercury-mercurous sulfate electrode (MSE +0.64 V vs. SHE, BASi, USA) and a silver macro-disc electrode (diameter of 2.52 mm, homemade) or a saturated calomel electrode (SCE +0.244 V vs. SHE, BASi Inc., Japan) and a platinum macro-electrode (diameter of 1.66 mm, BASi, USA) were used as combinations of reference and working electrodes. This is because that a slight leakage of chloride from a SCE can lead to AgCl deposition at a silver electrode when a corresponding potential is applied. Both electrodes were polished using a sequence of 1.0, 0.3 and 0.05 μm alumina lapping compounds (Bucher, Germany) prior to use. The electrochemical setup was thermostated at a constant value of 25.0 ± 0.2 °C. High purity N_2 flow (BOC Gases plc, U.K.) was used to remove oxygen from aqueous solutions as needed prior to the electrochemical measurements. Cyclic voltammetry (CV) was used to study the electrochemical behaviour of both working electrodes in either artificial or natural seawater. Prior to each voltammetric measurement when using a Ag macro-disc electrode, an initial 1-min electrochemical cleaning at −1.45 V vs MSE was conducted [46]. Square wave voltammetry (SWV) combined with standard additions was applied to determine the concentration of bromide using a Pt macro-disc electrode in either solution.

2.3. Sample collection and ion chromatography analysis

Three samples of natural seawater were studied. Two samples were collected from the L4 Station [51] in the English Channel (50° 15.00′ N, 4° 13.02′ W) at a depth of ca. 10 m, with one being collected in September 2020 and the other in October 2021. Another sample was collected off the coast of Dartmouth, Great Britain (50°20′N 3°32′W), at a depth of about 1 m in April 2022.500 mL of each sample was filter sterilised using 0.22 μm pore size Steritop filter units (Steritop Threaded Bottle Top Filter | SCGPS05RE (merckmillipore.com)) and was then kept refrigerated in the dark for the time leading up to these experiments. Ion chromatography measurements were made using a Dionex (Thermo Scientific, Sunnyvale, CA, USA) ICS-5000+ SP instrument. Separations were carried out using a Dionex IonPac AS23-4μm analytical column. The three samples of seawater were each diluted 200-fold with deionised water with a resistivity of 18.2 MΩ cm at 298 K prior to the analysis.

3. Results and discussion

In the following sections, we first use cyclic voltammetry to study the electrochemical behaviour of a silver macro-disc electrode for bromide detection both in chloride-free solutions and in the presence of chloride at hundred millimolar levels, the order of magnitude of which corresponds to the concentration levels in natural seawater. Whilst an amperometric or voltammetric approach for bromide detection is viable for pure bromide solutions or in the presence of low levels of other halide ions, in the presence of high chloride concentrations the bromide oxidation signal is found to be masked and the method fails. As an alternative voltammetric approach, the use of a platinum macro-disc electrode is explored and shown to be selective and sensitive enough for Br^- ion detection despite the presence of high levels of Cl^- in artificial seawater. Next, a sensitivity analysis is carried out in artificial seawater using the method of standard additions, while square wave voltammetry (SWV) with optimised parameters was applied to improve the sensitivity and precision. Finally, the bespoke method is applied for the quantitative analysis of bromide in three samples of natural seawater, the results of which are compared with that obtained by ion chromatography with good agreement being found.

3.1. Bromide detection using a silver macro-electrode

Bromide detection in the presence of the other halide ions, notably Cl^- and I^-, in an aqueous solution has been extensively studied using silver electrodes. For example, the selective determination of chloride and bromide ions in serum using cyclic voltammetry has been realised by Arai et al. who studied the behaviour of a silver macro-disc electrode in a PBS buffer with similar concentrations of halides (5 mM for Cl^-, 2 mM Br^- and 2 mM I^-) [48]. The measured CV indicated three clearly separated and well-defined redox peaks corresponding to the $Ag/AgCl/Cl^-$, $Ag/AgBr/Br^-$ and $Ag/AgI/I^-$ redox couples respectively. Meanwhile, silver nanowires [45] or nanoparticles [52] were also reported for successful selective halide measurements where voltammetric detections were conducted in solutions made of three halide ions with equal or similar concentrations, 5 mM in 0.1 M PBS for the former case and 80 μM for the latter. Hence as a starting point for bromide detection in seawater, we explored the possible selectivity of silver electrodes towards bromide in the presence of high chloride concentrations.

Following a 1-min electrochemical cleaning of a Ag macro-disc electrode at −1.45 V *vs.* MSE, cyclic voltammetric experiments, in which the potential sweep started at −0.90 V *vs.* MSE, swept towards −0.05 V before returning back to −0.90 V were conducted in a cell containing 0.1 M potassium nitrate and varying concentrations of potassium bromide (0.2, 0.4, 0.8, 1.2 and 1.6 mM). Each experiment was repeated three times. A control experiment was performed to analyse the behaviour of the silver electrode in the absence of bromide ions as shown by the black dashed line in Fig. 2 showing that no voltammetric signal was seen in a blank scan. In contrast, one anodic peak ($Peak_1$) with its reduction peak ($Peak_{1'}$) were observed when the measurement was conducted in bromide solutions with different concentrations (all the lines in Fig. 2 except the black dash line). The redox peaks shifted to a more negative positions as the bromide concentration increases. To be more specific, when the bromide concentration increased form 0.2 mM–1.6 mM, the potential of $Peak_1$ moved from −0.27 V to −0.33 V *vs.* MSE, and that of $Peak_{1'}$ moved from −0.42 V to −0.50 V *vs.* MSE. We infer that $Peak_1$ and $Peak_{1'}$ correspond to the following redox reaction, either reductive ($Peak_1$) or oxidative ($Peak_{1'}$):

$$Ag + Br^- \rightleftharpoons AgBr + e^- \quad (6)$$

The formal potential of the $Ag/AgBr/Br^-$ redox couple (eqn (6)) is reported to be −0.569 V *vs.* MSE [49], which allowing for the concentration of bromide being 1.6 mM is consistent with the data shown, noting that the MSE has a potential of 0.64 V *vs.* SHE [53]. The inset of Fig. 2 shows a plot of peak currents against concentrations of bromide,

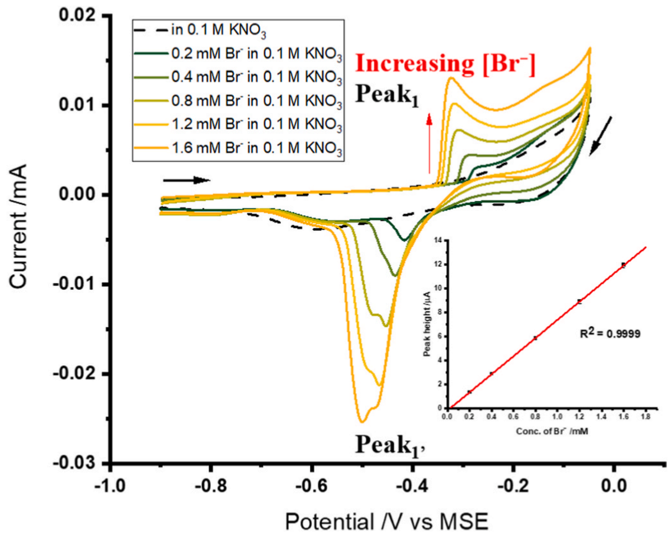

Fig. 2. Cyclic voltammograms measured at a scan rate of 20 mV s^{-1} using a Ag macro-electrode in degassed 0.1 M KNO_3 with different concentrations of Br^- (insert: calibration plot of the peak current of $Peak_1$ against the concentration of bromide ions). The start potential was −0.90 V vs. MSE.

which indicates a linear correlation (R^2 = 0.9999) between peak currents and bromide concentrations again consistent with the suggested assignment.

To study the effect of chloride ions, cyclic voltammetry was first conducted using a macro Ag electrode in a solution of 644 mM KCl. Then, voltammetric measurements were performed in solutions containing 0.84 mM Br^- ions with either 0.1 M KNO_3 or 644 mM KCl and in ASW. Note that the bromide and chloride concentrations are the recommended values for artificial seawater [50], as detailed in the Experimental Section. As indicated in Fig. 3, the voltammograms started at a potential of −0.90 V *vs.* MSE with a scan reversal at a potential of −0.20 V *vs.* MSE, back to the starting potential. $Peak_2$ at −0.34 V and $Peak_{2'}$ at −0.56 V *vs.* MSE were observed in a solution containing KCl only (red line), We assign $Peak_2$ and $Peak_{2'}$ to the following redox chemistry:

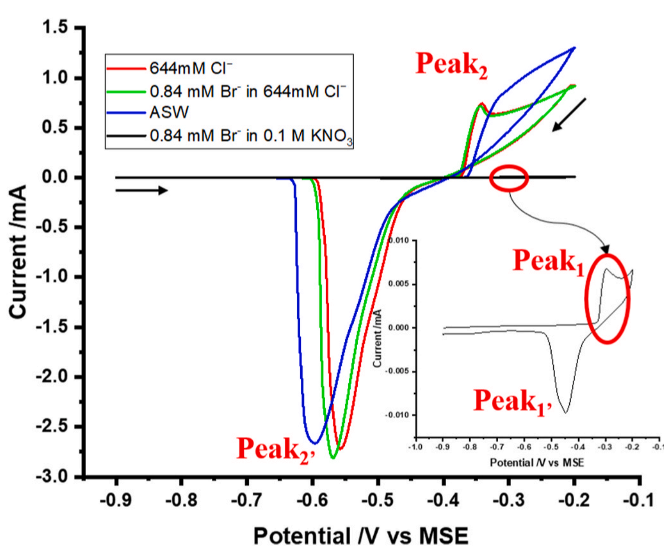

Fig. 3. Cyclic voltammograms at a scan rate of 20 mV s^{-1} using a Ag macro-electrode in degassed 644 mM Cl^- (red line), 0.84 mM Br^- with 644 mM KCl (green line), ASW containing 0.84 mM Br^- and 644 mM Cl^- (blue line) and 0.84 mM Br^- with 0.1 M KNO_3 (black line). The start potential was −0.90 V vs. MSE. (For interpretation of the references to colour in this figure legend, the reader is referred to the Web version of this article.)

$$Ag + Cl^- \rightleftharpoons AgCl + e^- \quad (7)$$

which is consistent with the formal potential of the Ag/AgCl/Cl^- couple reported as −0.418 V *vs.* MSE [49]. On adding 0.84 mM KBr (green line), there was no perceptible change in the peak potentials of Peaks 2 and 2'. Voltammetry in ASW (blue line) resulted in a broader redox couple, with an oxidation peak at about −0.32 V and a reduction peak at −0.60 V *vs.* MSE. Accordingly, the redox peaks labelled Peaks 2 and 2′ in Fig. 3 recorded with the addition of 0.84 mM Br^- are again attributed to the Ag/AgCl/Cl^- couple, while the broad peak shape obtained in ASW reflects the deposition from and stripping into the more complex matrix. Note that the crossover detected on the back sweep in the three chloride-containing solutions results from surface nucleation of the new AgCl phase so that increased currents flow after more nuclei are formed. $Peak_1$ at −0.30 V and its back $Peak_{1'}$ at −0.45 V *vs.* MSE were seen in a solution consisting of 0.84 mM Br^- and 0.1 M KNO_3, and are attributed to the Ag/AgBr/Br^- redox couple as above (black line in Fig. 3). However, for the case of 644 mM chloride ions, and the ASW (green line and blue line in Fig. 3), the strong current even at relative low oxidising potentials from the formation of AgCl ($Peak_2$) when the potential applied was higher than about −0.38 V fully masked the Ag/AgBr/Br^- signals ($Peak_1$ and $Peak_{1'}$) on both the oxidative and reductive scans. Thus, whilst silver electrodes can be used to detect bromide in the presence of similar concentrations of chloride, when an excess of the latter is present, Peaks 1 and 1′ cannot be used analytically. It is thus not possible to use a silver electrode for bromide detection in seawater. As an alternative, the use of a Pt macro-disc electrode was explored as reported in the following sections.

3.2. Electrochemical study of Br^- with a Pt macro-electrode

In this section, a Pt macro-disc electrode is applied to study its electrochemical behaviour towards bromide ions, especially in the presence of Cl^- at hundred millimolar levels in ASW. The study was first carried out in a degassed solution of 0.84 mM Br^- ions with 0.1 M KNO_3 to fingerprint the bromide peak. Cyclic voltammogram with different scan rates of 20, 50, 100, 200 and 400 mVs^{-1}, of which the potential started at 0 V *vs.* SCE, swept towards 1.7 V before returning to 0 V, were recorded as shown in Fig. 4 (a). One oxidation peak at 0.98 V *vs.* SCE and one reduction peak at 0.85 V *vs.* SCE were observed at different scan rates, consistent with the observations of Chen, Kumar et al. [54]. We infer that Peak 1 (oxidation) and Peak 1' (reduction) correspond to the following redox reaction:

$$Br^- \rightleftharpoons \frac{1}{2}Br_2 + e^- \quad (8)$$

Note that at the concentrations of bromide used, the formation of the tribromide anion is negligible [54]. The inset to Fig. 4 (a) shows that the peak current scales with the square root of the voltage scan rate. The linearity confirms a diffusion-controlled electrode process. The diffusion coefficient of the bromide ion in 0.1 M KNO_3 (see SI, Section 1 and 2) was measured based on the Randles–Ševčík equation for a simple irreversible one-electron transfer oxidation giving a value of 2.1 × 10^{-5} cm^2/s which compares well with the literature value of 2.08 × 10^{-5} cm^2/s [55].

To study the response of Pt electrodes towards bromide in ASW, cyclic voltammetric experiments starting at 0 V *vs.* SCE, swept towards 1.7 V and back to 0 V were again employed in degassed ASW and ASW containing no Br^- at a scan rate of 20 mVs^{-1} (blue line and red line in Fig. 4 (b)). The ASW voltammogram is dominated by the oxidation of chloride (Peak 2) and the reduction of Cl_2 on the reverse scan. The oxidation peak is seen at 1.33 V *vs.* SCE (Peak 2) with a corresponding reduction peak at around 0.96 *vs.* SCE (Peak 2'), consistent with: the mid-potential of which (1.39 *vs.* SHE) agrees with the literature being 1.40 *vs.* SHE [49].

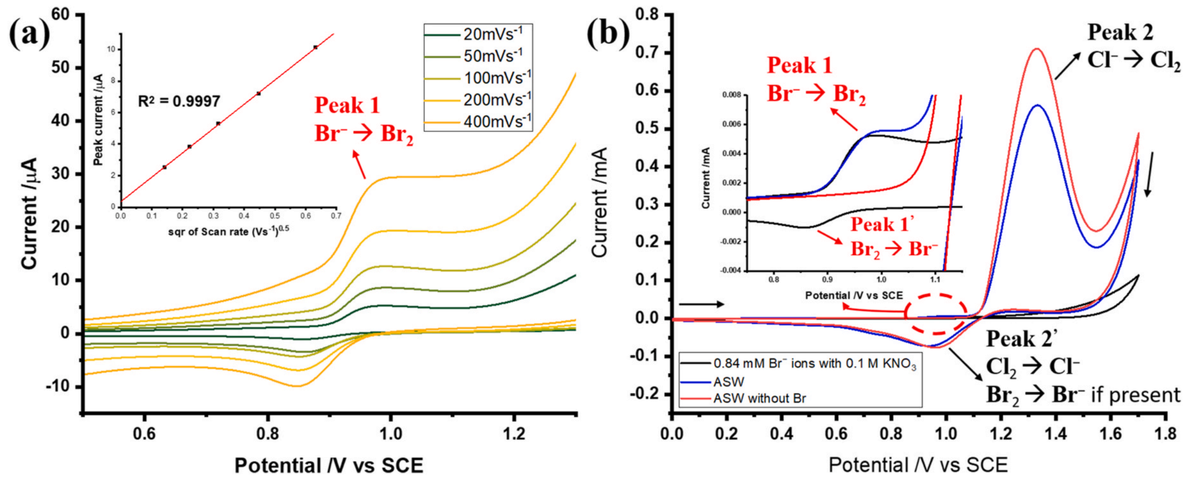

Fig. 4. (a) Cyclic voltammograms in degassed 0.84 mM Br^- with 0.1 M KNO_3 at variable scan rates of 20, 50, 100, 200 and 400 mV s^{-1}. The inset shows the plot of peak currents of bromide peak as a function of the square root of scan rate. See text for details of the scan range and the start potential. (b) Cyclic voltammograms for Br^- detection using a Pt macro-electrode at a scan rate of 20 mV s^{-1} in degassed 0.84 mM Br^- in 0.1 M KNO_3 (black line), ASW (blue line) and ASW without Br (red line). The inset shows the enlarged CV focusing on bromide redox peaks. See text for details of the scan range and the start potential. (For interpretation of the references to colour in this figure legend, the reader is referred to the Web version of this article.)

$$Cl^- \rightleftharpoons \frac{1}{2}Cl_2 + e^- \tag{9}$$

As shown in the insert of Fig. 4 (b), Peak 1 attributed to the oxidation Br^- was still clearly resolved in ASW (blue line), while it was not seen in the absence of bromide (red line). Meanwhile, Peak 2 related to the

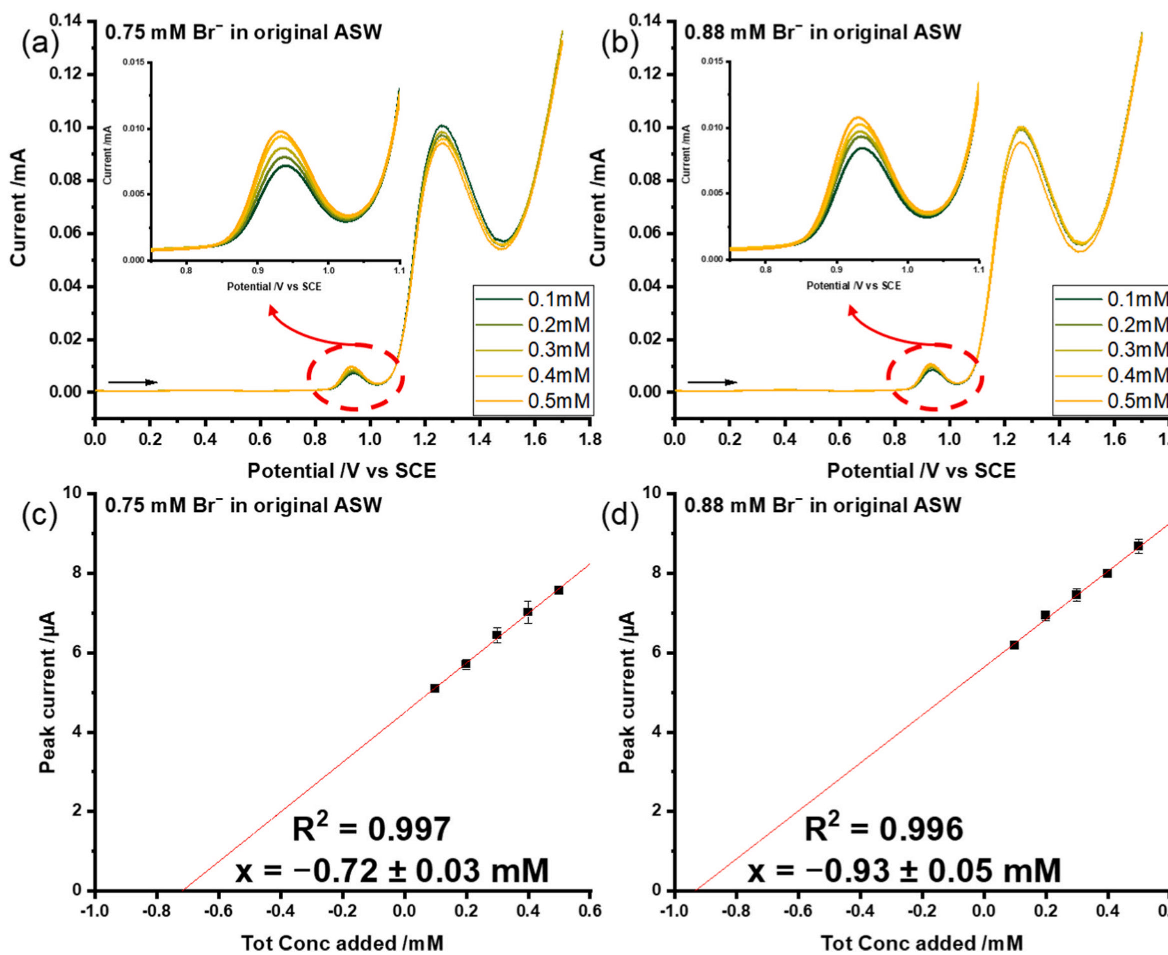

Fig. 5. Square wave voltammograms (frequency 50 Hz, step potential 1 mV, and amplitude 10 mV) recorded at a macro-Pt electrode in degassed ASW with original bromide concentrations of (a) 0.75 mM and (b) 0.88 mM (the inset shows enlarged SWVs with a potential window from 0.75 to 1.10 V, focusing on the bromide peak); see text for details of the scan range and the start potential. Graphical analysis of standard additions to ASW with an original bromide concentration of (c) 0.75 mM and (d) 0.88 mM with variable total volume.

oxidation Cl^- obtained in ASW (blue line) has a peak height lower than that in ASW without presence of bromide (red line). This is likely explained by the following. First, the oxidation of bromide occurs at a lower potential (0.98 V *vs.* SCE) than that of chloride (1.33 V *vs.* SCE), so that the process at peak 1 has consumed some of the silver, causing less charge to be passed under peak 2. Secondly, due to the finite surface area of the silver working electrode, the blockage of its surface by AgBr in ASW results to less area available for the AgCl deposition.

So, to conclude, importantly, the signal of oxidation of Cl^- does not mask the oxidation peak of bromide when voltammetry is conducted in ASW when studied with a Platinum electrode. Thus, a Pt macro-disc electrode was evidenced to be suitable for further sensitivity analysis of bromide ions in ASW and natural seawater.

3.3. Sensitivity analysis by standard additions using SWV

In this section, the electroanalytical responses of bromide ions in the presence of high levels of chloride, namely in ASW, were explored on a Pt macro-disc electrode. Standard additions were used since it is recognised as especially appropriate when the sample composition is unknown and/or complex and affects the analytical signal [38]. To obtain the best-defined square wave voltammograms for sensitivity analysis, the optimisation of SWV parameters, including frequency, step potential and amplitude, was implemented in a degassed ASW (SI, Section 3). The optimised SWV with a frequency of 50 Hz, amplitude of 10 mV and step potential of 1 mV was then applied in two ASW solutions with different concentrations of bromide corresponding to the usual extreme limits of 0.75 and 0.88 mM encountered in natural seawater [5,56] to explore the sensitivity of detection. As shown in Fig. 5a and b, voltammograms were performed starting at a potential of 0 V *vs.* SCE, and stopping at 1.7 V *vs.* SCE for an oxidative scan. The insets show enlarged SWVs with a potential window from 0.75 to 1.10 V, focusing on the bromide peak. Additions of 0.1–0.5 mM KBr to two ASW solutions were conducted. The measurements in the mixture with each addition were repeated three times. There are two oxidation peaks, namely of bromide (0.94 V *vs.* SCE) and of chloride (1.26 V *vs.* SCE), observed at similar potentials as in the CVs (Fig. 4b). To analyse the data, the oxidation peak currents of the bromide were recorded. The plots of peak current against the concentration of bromide added to original ASW samples with 0.75 mM and 0.88 mM Br^- are shown in Fig. 5c and d respectively. Both showed good linearity. The intercept on the x-axis corresponds to the unknown initial concentration of the analyte [38]. Therefore, the intercepts of -0.72 ± 0.03 mM obtained from Fig. 5c and -0.93 ± 0.05 mM from Fig. 5d provide a good agreement with the original bromide concentrations in the ASW samples.

3.4. Real sample analysis

As discussed in the last section, SWV combined with the standard addition method is appropriate for determining the bromide concentration in ASW. To assess the reliability and feasibility of SWV for the electrochemical analysis of real samples, the analysis of three different real samples was performed. Two samples were collected from the L4 Station [51] in the English Channel (50° 15.00′ N, 4° 13.02′ W) at a depth of ca. 10 m, with one being collected in September 2020 (Sample 1) and the other in October2021 (Sample 2). Another sample was collected off the coast of Dartmouth, Great Britain (50°20′N 3°32′W), at a depth of about 1 m in April 2022 (Sample 3). Each sample was filter sterilised using 0.22 μm pore size Steritop filter units and was then kept refrigerated in the dark in the time leading up to these experiments. Ion chromatography measurements were made to independently study the composition of the three samples, the results of which are summarised in SI, Table S1. The concentrations of bromide obtained by IC are compared below with the values measured electrochemically.

Cyclic voltammetry using a Pt macro-disc electrode was used to study the three degassed samples of natural seawater. As shown in Fig. 6,

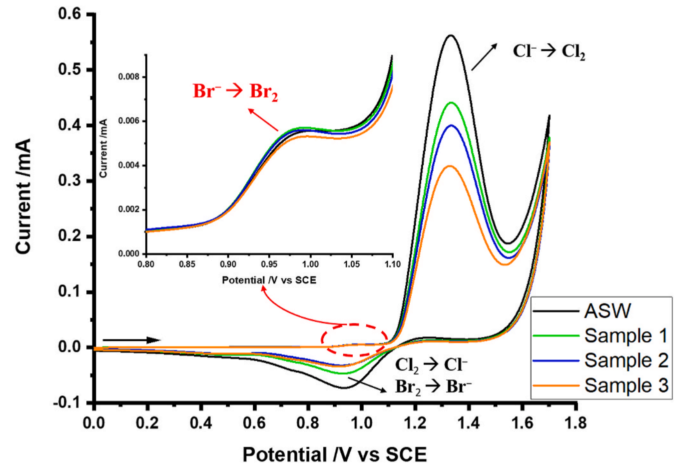

Fig. 6. Cyclic voltammograms for Br^- detection using a Pt macro-electrode at a scan rate of 20 mV s^{-1}. The start potential was 0 V vs SCE with measurements made in degassed ASW (black line), sample 1 (green line), sample 2 (blue line), and sample 3 (orange line); the inset shows the zoomed CV focusing on bromide oxidation peaks. (For interpretation of the references to colour in this figure legend, the reader is referred to the Web version of this article.)

the scans start at 0 V *vs.* SCE, sweep towards 1.7 V before returning to 0 V. The voltammograms obtained in three natural samples (green, blue and orange lines) have the same voltammetric features as were observed in ASW (black line). To reiterate, the oxidation peak at ca 0.99 V *vs.* SCE corresponds to bromide oxidation (see insert) and the one at 1.33 V *vs.* SCE corresponds to chloride oxidation, with a reduction peak seen at ca 0.93 V *vs.* SCE.

Then, three independent analyses were performed for each sample using SWV and the method of standard additions as described in the last section. SWV with the previously optimised parameters of a frequency of 50 Hz, amplitude of 10 mV and step potential of 1 mV was applied and additions of 0.1–0.5 mM KBr to each of them were conducted. As shown in Fig. 7a, b and 7c, voltammograms were conducted starting at a potential of 0 V *vs.* SCE, and stopping at 1.7 V *vs.* SCE for an oxidative scan. There are two oxidation peaks, namely of bromide (ca 0.93 V *vs.* SCE) and of chloride (ca 1.26 V *vs.* SCE), observed at similar potentials as in ASW (Fig. 5a and b). To analyse the data, the oxidation peak currents of the bromide were recorded as a function of additions of bromide. The plots of peak current against the concentration of bromide added to original natural seawater samples are shown in Fig. 7d, e and 7f respectively and display good linearity. Table 3 summarises the intercepts on the x axis, corresponding to the unknown initial concentrations of bromide in the three samples, and are compared with that measured by IC. Clearly, the developed electrochemical analysis results in a good agreement with IC, even for sample 1 containing bromide ions with a concentration higher than the expected value in natural seawater.

4. Conclusions

Though literature shows that silver electrodes can be used for bromide detection in the presence of similar concentrations of chloride [45,48,52], the bromide signal obtained in seawater is masked by the much larger chloride signal as reported above. Thus, the use of a Pt macro-disc electrode as an alternative was explored in artificial seawater first, followed by analysis of real seawater samples. By employing SWV to improve the sensitivity and using the standard addition method, a selective quantification of bromide ions can not only be achieved in ASW, but also in natural seawater, despite the high concentration of chloride and the highly complex matrix that is seawater. The obtained concentration of bromide in each sample shows a good match with that measured by ion chromatography, which indicates that electrochemistry may offer a better option with the benefits of low cost, simplicity

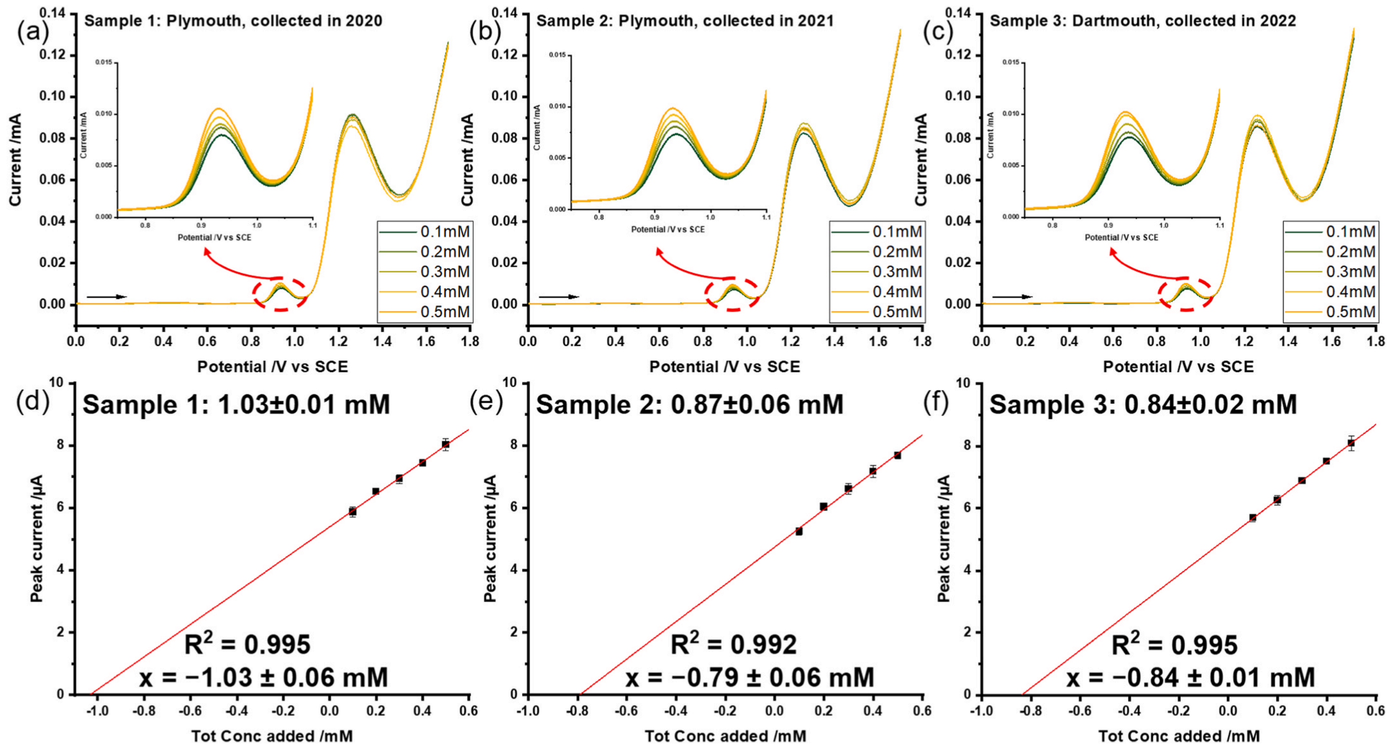

Fig. 7. Square wave voltammograms (frequency 50 Hz, step potential 1 mV, and amplitude 10 mV) recorded using a macro-Pt electrode in degassed (a) sample 1, (b) sample 2 and (c) sample 3 (the inset shows enlarged SWVs, focusing on bromide peak); see text for details of the scan range and the start potential. Graphical treatment of standard additions to (d) sample 1, (e) sample 2 and (f) sample 3 with variable total volume.

Table 3
Comparison of the measured bromide concentrations in three natural seawater samples.

	Measured Concentration using SWV/mM	Measured Concentration using IC/mM
Sample 1	1.03 ± 0.06	1.03 ± 0.01
Sample 2	0.79 ± 0.06	0.87 ± 0.06
Sample 3	0.84 ± 0.01	0.84 ± 0.02

and rapidity with comparable selectivity for bromide detection in seawater.

Credit author statement

Yuqi Chen: Validation, Formal analysis, Investigation, Writing – original draft, Visualization, **Prof Richard G. Compton:** Writing – review & editing, Supervision, Project administration, Funding acquisition, Conceptualization, Methodology, Resources

Declaration of competing interest

The authors declare that they have no known competing financial interests or personal relationships that could have appeared to influence the work reported in this paper.

Data availability

Data will be made available on request.

Acknowledgement

We appreciate the gift of samples of Plymouth seawater collected by Dr. Samuel Barton and Angela Ward (at MBA, Plymouth) and the gift of sample of Dartmouth seawater sample donated by Dr. Craig Dedman.

Appendix A. Supplementary data

Supplementary data to this article can be found online at https://doi.org/10.1016/j.talanta.2022.124019.

References

[1] F.R. Spellman, The Handbook of Nature, Bernan Press, 2019.
[2] F. Chai, K.S. Johnson, H. Claustre, X. Xing, Y. Wang, E. Boss, S. Riser, K. Fennel, O. Schofield, A. Sutton, Monitoring ocean biogeochemistry with autonomous platforms, Nat. Rev. Earth Environ. 1 (6) (2020) 315–326.
[3] H.K. Lotze, D.P. Tittensor, A. Bryndum-Buchholz, T.D. Eddy, W.W.L. Cheung, E. D. Galbraith, M. Barange, N. Barrier, D. Bianchi, J.L. Blanchard, L. Bopp, M. Büchner, C.M. Bulman, D.A. Carozza, V. Christensen, M. Coll, J.P. Dunne, E. A. Fulton, S. Jennings, M.C. Jones, S. Mackinson, O. Maury, S. Niiranen, R. Oliveros-Ramos, T. Roy, J.A. Fernandes, J. Schewe, Y.-J. Shin, T.A.M. Silva, J. Steenbeek, C.A. Stock, P. Verley, J. Volkholz, N.D. Walker, B. Worm, Global ensemble projections reveal trophic amplification of ocean biomass declines with climate change, Proc. Natl. Acad. Sci. U.S.A. 116 (26) (2019) 12907–12912.
[4] U.S. Environmental Protection Agency, Accessed on 6 December 2021 2021, https://www.epa.gov/ocean-acidification/understanding-science-ocean-and-coastal-acidification, 2021.
[5] K. Uraisin, T. Takayanagi, M. Oshima, D. Nacapricha, S. Motomizu, Kinetic-spectrophotometric method for the determination of trace amounts of bromide in seawater, Talanta 68 (3) (2006) 951–956.
[6] S.-M. Fan, D.J. Jacob, Surface ozone depletion in Arctic spring sustained by bromine reactions on aerosols, Nature 359 (6395) (1992) 522–524.
[7] A.C. Leri, S.C. Myneni, Natural organobromine in terrestrial ecosystems, Geochem. Cosmochim. Acta 77 (2012) 1–10.
[8] X. Wei, M. Yang, Q. Zhu, E.D. Wagner, M.J. Plewa, Comparative quantitative toxicology and QSAR modeling of the haloacetonitriles: forcing agents of water disinfection byproduct toxicity, Environ. Sci. Technol. 54 (14) (2020) 8909–8918.
[9] J.M. Allen, M.J. Plewa, E.D. Wagner, X. Wei, K. Bokenkamp, K. Hur, A. Jia, H. K. Liberatore, C.-F.T. Lee, R. Shirkhani, S.W. Krasner, S.D. Richardson, Drivers of

disinfection byproduct cytotoxicity in U.S. drinking water: should other DBPs be considered for regulation? Environ. Sci. Technol. 56 (1) (2022) 392–402.
[10] P.S. Heckerling, K.A. Ammar, Bromide intoxication due to propantheline bromide, Am. J. Nephrol. 16 (6) (1996) 537–539.
[11] S. Suzuki, K. Kawakami, F. Nakamura, S. Nishimura, K. Yagi, M. Seino, Bromide, in the therapeutic concentration, enhances GABA-activated currents in cultured neurons of rat cerebral cortex, Epilepsy Res. 19 (2) (1994) 89–97.
[12] M.E. Pilson, An Introduction to the Chemistry of the Sea, Cambridge University Press, 2012.
[13] E.L. Lewis, The practical salinity scale of 1978 and its antecedents, Mar. Geodes. 5 (4) (1982) 350–357.
[14] G.S. Lagerloef, C.T. Swift, D.M. Le Vine, Sea surface salinity: the next remote sensing challenge, Oceanography 8 (2) (1995) 44–50.
[15] J.J. Morgan, W. Stumm, Aquatic Chemistry-An Introduction Emphasizing Chemical Equilibria in Natural Waters, John Wiley & Sons, New York, NY, 1981.
[16] E. Salameh, A. Tarawneh, M. Al-Raggad, Origin of high bromide concentration in the water sources in Jordan and in the Dead Sea water, Arabian J. Geosci. 9 (5) (2016) 1–20.
[17] D.R. Jones, Applying the phenol red colorimetric method for bromide analysis to reducing waters, Talanta 40 (1) (1993) 43–51.
[18] P.I. Anagnostopoulou, M.A. Koupparis, Automated flow-injection phenol red method for determination of bromide and bromide salts in drugs, Anal. Chem. 58 (2) (1986) 322–326.
[19] W.J.M. Emaus, H.J. Henning, Determination of bromide in sodium chloride matrices by flow-injection analysis using blank peak elimination and kinetic discrimination, Anal. Chim. Acta 272 (2) (1993) 245–250.
[20] K. Uraisin, D. Nacapricha, S. Lapanantnoppakhun, K. Grudpan, S. Motomizu, Determination of trace amounts of bromide by flow injection/stopped-flow detection technique using kinetic-spectrophotometric method, Talanta 68 (2) (2005) 274–280.
[21] N. Yonehara, S.-i. Chaen, T. Tomiyasu, H. Sakamoto, Flow injection-spectrophotometric determination of trace amounts of bromide by its catalytic effect on the 4,4'-bis(dimethylamino)diphenylmethane-chloramine T reaction, Anal. Sci. 15 (3) (1999) 277–281.
[22] S. M.R., J.R. Elah, Kinetic spectrophotometric method for trace amounts determination of bromide in pharmaceutical samples using Janus Green-Bromate system, Int. J. Ind. Chem. 2 (1) (2011) 27–32.
[23] A. Sheibani, M.R. Shishehbore, Z.T. Ardakani, Kinetic spectrophotometric determination of bromide in clidinium-c drug, Chin. Chem. Lett. 22 (5) (2011) 595–598.
[24] H. Akaiwa, H. Kawamoto, M. Osumi, Simultaneous determination of bromide and chloride in natural waters by ion-exchange chromatography and direct potentiometry with an ion-selective electrode, Talanta 29 (8) (1982) 689–690.
[25] S. Seefeld, U. Baltensperger, Determination of bromide in snow samples by ion chromatography with electrochemical detection, Anal. Chim. Acta 283 (1) (1993) 246–250.
[26] H. Fabre, M.D. Blanchin, N. Bosc, Capillary electrophoresis for the determination of bromide, chloride and sulfate as impurities in calcium acamprosate, Anal. Chim. Acta 381 (1) (1999) 29–37.
[27] O. Stålberg, K. Sander, C. Sänger-van de Griend, The determination of bromide in a local anaesthetic hydrochloride by capillary electrophoresis using direct UV detection, J. Chromatogr. A 977 (2) (2002) 265–275.
[28] J.P. Pascali, M. Trettene, F. Bortolotti, G.d. Paoli, R. Gottardo, F. Tagliaro, Direct analysis of bromide in human serum by capillary electrophoresis, J. Chromatogr. B 839 (1) (2006) 2–5.
[29] K. Fukushi, K. Watanabe, S. Takeda, S.-I. Wakida, M. Yamane, K. Higashi, K. Hiiro, Determination of bromide ions in seawater by capillary zone electrophoresis using diluted artificial seawater as the buffer solution, J. Chromatogr. A 802 (1) (1998) 211–217.
[30] N. Kocatürk, N. Öztekin, F. Bedia Erim, Direct determination of bromide ions in seawater by capillary zone electrophoresis using polyethyleneimine-coated capillaries, Anal. Bioanal. Chem. 377 (7) (2003) 1207–1211.
[31] G. Rechnitz, M. Kresx, Potentiometric measurements with choride-sensitive and bromide-sensitive membrane electrodes, Anal. Chem. 38 (12) (1966) 1786–1788.
[32] E.M. Zahran, Y. Hua, Y. Li, A.H. Flood, L.G. Bachas, Triazolophanes: a new class of halide-selective ionophores for potentiometric sensors, Anal. Chem. 82 (1) (2010) 368–375.
[33] Ö. Isildak, O. Özbek, K. Yigit, A bromide-selective PVC membrane potentiometric sensor, Bulg. Chem. Commun. 52 (4) (2020) 448–452.
[34] D. Vlascici, N. Plesu, G. Fagadar-Cosma, A. Lascu, M. Petric, M. Crisan, A. Belean, E. Fagadar-Cosma, Potentiometric sensors for iodide and bromide based on Pt(II)-Porphyrin, Sensors 18 (7) (2018) 2297.
[35] L. Pittwell, The determination of hydroxylamine in Ethiopian rivers and lakes, Microchim. Acta 64 (4) (1975) 425–429.
[36] J.H. Butler, J.E. Pequegnat, L.I. Gordon, R.D. Jones, Cycling of methane, carbon monoxide, nitrous oxide, and hydroxylamine in a meromictic, coastal lagoon, Estuarine, Coastal Shelf Sci 27 (2) (1988) 181–203.
[37] K.C. Thompson, P. Quevauviller, Analytical Methods for Drinking Water: Advances in Sampling and Analysis, John Wiley & Sons, 2005.
[38] D.C. Harris, Quantitative Chemical Analysis, Macmillan, 2010.
[39] G.G. Mohamed, T.A. Ali, M.F. El-Shahat, A.M. Al-Sabagh, M.A. Migahed, New screen-printed ion-selective electrodes for potentiometric titration of cetyltrimethylammonium bromide in different civilic media, Electroanalysis 22 (21) (2010) 2587–2599.
[40] G.A. Rechnitz, M.R. Kresx, Potentiometric measurements with choride-sensitive and bromide-sensitive membrane electrodes, Anal. Chem. 38 (12) (1966) 1786–1788.
[41] NT Sensors, Bromide Ion Selective Electrode (ISE), 2022 (Accessed June 24th 2022), https://www.ntsensors.com/parameters/bromide-ion-selective-electrode/#tab-id-2.
[42] einstein™ Sensors, Bromide Sensor (Accessed June 24th 2022), http://einsteinworld.com/product/bromide-sensor/.
[43] Electro-chemical devices, bromide sensor (Accessed June 24th 2022), https://ecdi.com/portfolio-item/bromide-sensors.
[44] J. Milikić, I. Stoševski, J. Krstić, Z. Kačarević-Popović, Š. Miljanić, B. Šljukić, Electroanalytical sensing of bromides using radiolytically synthesized silver nanoparticle electrocatalysts, J. Anal. Methods Chem. 2017 (2017), 2028417.
[45] X. Qin, H. Wang, Z. Miao, X. Wang, Y. Fang, Q. Chen, X. Shao, Synthesis of silver nanowires and their applications in the electrochemical detection of halide, Talanta 84 (3) (2011) 673–678.
[46] Y. Guo, R.G. Compton, A bespoke chloride sensor for seawater: simple and fast with a silver electrode, Talanta 232 (2021), 122502.
[47] X. Qin, Z. Miao, X. Du, Q. Chen, Electrocatalytic activation of silver nanowires-modified Pt electrode by cyclic voltammetry in comparison with differential pulse voltammetry in halide determination, Electroanalysis 28 (3) (2016) 555–561.
[48] K. Arai, F. Kusu, N. Noguchi, K. Takamura, H. Osawa, Selective determination of chloride and bromide ions in serum by cyclic voltammetry, Anal. Biochem. 240 (1) (1996) 109–113.
[49] A. Bard, Standard Potentials in Aqueous Solution, Routledge, 2017.
[50] F.M.M. Morel, J.G. Rueter, D.M. Anderson, R.R.L. Guillard, Aquil: a chemically defined phytoplankton culture medium for trace metal studies, J. Phycol. 15 (2) (1979) 135–141.
[51] T.J. Smyth, J.R. Fishwick, L. AL-Moosawi, D.G. Cummings, C. Harris, V. Kitidis, A. Rees, V. Martinez-Vicente, E.M.S. Woodward, A broad spatio-temporal view of the Western English Channel observatory, J. Plankton Res. 32 (5) (2009) 585–601.
[52] J. Bujes-Garrido, D. Izquierdo-Bote, A. Heras, A. Colina, M.J. Arcos-Martínez, Determination of halides using Ag nanoparticles-modified disposable electrodes. A first approach to a wearable sensor for quantification of chloride ions, Anal. Chim. Acta 1012 (2018) 42–48.
[53] K. Tsuji, P.J. Elving, Conversion of polarographic and other potentials from one reference electrode to another, Anal. Chem. 41 (1) (1969) 216–&.
[54] H. Chen, A. Kaliyaraj Selva Kumar, H. Le, R.G. Compton, Non-unity stoichiometric reversible electrode reactions. The effect of coupled kinetics and the oxidation of bromide, J. Electroanal. Chem. 876 (2020), 114730.
[55] R.E. White, S.E. Lorimer, A model of the bromine/bromide electrode reaction at a rotating disk electrode, J. Electrochem. Soc. 130 (5) (1983) 1096–1103.
[56] K.K. Turekian, The fate of metals in the oceans, Geochem. Cosmochim. Acta 41 (8) (1977) 1139–1144.